Available online at www.sciencedirect.com
ScienceDirect
Chinese Journal of Natural Medicines 2022, **20**(3): 229-240
doi: 10.1016/S1875-5364(22)60159-6
Chinese Journal of Natural Medicines

•Research article•

Design and semisynthesis of oleanolic acid derivatives as VEGF inhibitors: Inhibition of VEGF-induced proliferation, angiogenesis, and VEGFR2 activation in HUVECs

MENG Ning[1*], XIE Hong-Xu[1], HOU Jia-Rong[1], CHEN Yan-Bin[1], WU Meng-Jun[2], GUO Yue-Wei[2*], JIANG Cheng-Shi[1*]

[1] *School of Biological Science and Technology, University of Jinan, Jinan 250022, China;*
[2] *State Key Laboratory of Drug Research, Shanghai Institute of Materia Medica, Chinese Academy of Sciences, Shanghai 201203, China*

Available online 20 Mar., 2022

[ABSTRACT] Angiogenesis inhibitors targeting the VEGF signaling pathway are developed into drugs for the treatment of vaious diseases, such as cancer, rheumatoid arthritis, and age-related macular degeneration. Recent studies have revealed that oleanolic acid (OA), a natural pentacyclic triterpenoid, inhibited the VEGF/VEGFR2 signaling pathway and angiogenesis in HUVECs, which may represent an attractive VEGF inhibitor. In this paper, rational structural modification towards OA was performed in order to improve its inhibitory effects aganist VEGF and anti-angiogenesis potential. As a result, a series of novel OA derivatives, possessing α,β-unsaturated ketone system in ring A and amide functional group at C-28, were prepared and evaluated for cytotoxicity and their ability to inhibit VEGF-induced abnormal proliferation of HUVECs. The results showed that two promising derivatives, OA-1 and OA-16, exhibited no *in vitro* cytotoxicity against HUVECs but showed more potent inhibitory activity against VEGF-induced proliferation and angiogenesis in HUVECs, compared with OA. The results of Western blot indicated that OA-1 and OA-16 inhibited VEGF-induced VEGFR2 activation. Furthermore, small interfering RNA experiments were performed to confirm that both compounds inhibited VEGF-induced angiogenesis *via* VEGFR2. Thus, the present study resulted in the discovery of new promising OA-inspired VEGF inhibitors, which can serve as potential lead compounds for the treatment of angiogenesis-related diseases.

[KEY WORDS] Oleanolic acid; Structural modification; VEGF inhibitor; VEGFR2; Angiogenesis
[CLC Number] R284.3, R965 **[Document code]** A **[Article ID]** 2095-6975(2022)03-0229-12

Introduction

Vascular endothelial growth factor (VEGF) is a key angiogenic factor, and related to the pathogenesis and progress of several diseases, including cancer, rheumatoid arthritis, and age-related macular degeneration [1-3]. Specifically acting on vascular endothelial cells, VEGF plays an important role in the formation of new blood vessels that results in stimulation of proliferation, migration, survival and permeability of endothelial cells [4-7]. VEGF was referred as a validated target for anti-angiogenesis and anti-cancer treatment [8-9]. VEGF inhibitors targeting proliferating endothelial cells were expected to be less toxic than conventional anticancer drugs [10]. In recent years, numerous VEGF-targeted small molecule inhibitors or nonclonal antibodies have been brought to market [11-13]. Notably, about ten small molecule VEGF inhibitors (sunitinib and pazopanib, etc.) had been approved for the treatment of cancer [14].

Natural products are an important source for new drug discovery, especially in the area of anti-cancer drugs. According to previous reports, approximate 83% of 185 small anticancer drugs approved from 1981 to 2019 were directly or indirectly derived from natural products [15]. Oleanolic acid

[Received on] 16-Sep.-2021
[Research funding] This work was supported by the National Natural Science Foundation of China (Nos. 21672082 and 31671214), the Natural Science Foundation of Shandong Province (Nos. ZR2019YQ31, ZR2020YQ52, and ZR2020MB103), the Project of Shandong Province Higher Educational Youth Innovation Science and Technology Program (No. 2020KJE006), and the Science and Technology Project of University of Jinan (No. XKY2004).
[*Corresponding author] E-mails: mls_mengn@ujn.edu.cn (MENG Ning); ywguo@simm.ac.cn (GUO Yue-Wei); bio_jiangcs@ujn.edu.cn (JIANG Cheng-Shi)
These authors have no conflict of interest to declare.

(OA, Fig. 1) is a natural pentacyclic triterpenoid isolated from many edible and medicinal plants [16-17]. OA and its derivatives have been reported to display various pharmacological effects, such as anti-cancer, anti-inflammatory, and anti-diabetic activities [18-25]. However, the underlying mechanism of OA has not been fully understood. Recently, OA has been found to inhibit VEGF-induced VRGFR-2 activation and angiogenesis in HUVECs without cytotoxicity, indicating its anti-cancer potential by targeting the VEGF pathway [26]. Therefore, the current research was aimed to improve OA's inhibitory activitiy against VEGF and antiangiogenic potential by structural modification. Previous reports indicated that the introduction of functional groups at the C-28 carboxyl group usually improved the bioactivity and physicochemical characteristics of OA. Thus the carboxylic acid was modified through amidation to evaluate its effect on inhibitory activitiy against VEGF and antiangiogenic potential. Furthermore, the *α*,*β*-unsaturated ketone (Michael acceptor) pharmacophore, which form adducts with reactive thiol groups of proteases resulting in modification and misfolding of protein, was widely present in the anti-tumor compounds or drugs [27-30]. Based on these observations, it was hypothesized that the introduction of Michael acceptor in ring A and amide moiety at C-28 can stimulate the increases in inhibitory activity against VEGF, and a series of OA derivatives (Fig. 2) were designed and prepared as shown in Fig. 2. Herein, we reported the synthesis of OA-derived VEGF inhibitors, their *in vitro* cytotoxicities and the inhibitory activity against VEGF-induced proliferation, angiogenesis, and VEGFR2 activation in HUVECs.

Results and Discussion

Chemistry

The synthetic route of OA derivatives was shown in Fig. 2. Briefly, OA as starting material was oxidized with 2-iodoyl benzoic acid (IBX) to obtain OA-CO_2H, which was then reacted with 1-[bis(dimethylamino)methylene]-1*H*-1,2,3-triazolo[4,5-*b*]pyridinium 3-oxid hexafluorophosphate (HATU) to produce the intermediate OA-HATU. Finally, the target compounds OA-1−OA-16 were prepared through reaction of OA-HATU with the corresponding amines. The structures of all compounds were confirmed by analysis of their ^1H, ^{13}C NMR and HRESIMS spectra, which were included in the supplementary materials.

Compounds OA-1 and OA-16 exhibited no significant effect on HUVEC growth but inhibited the proliferation of VEGF-induced HUVECs

The inhibitory activity against VEGF and antiangiogenic potential of OA derivatives were evaluated by a cell-based assay to screen out the compounds with superior activity

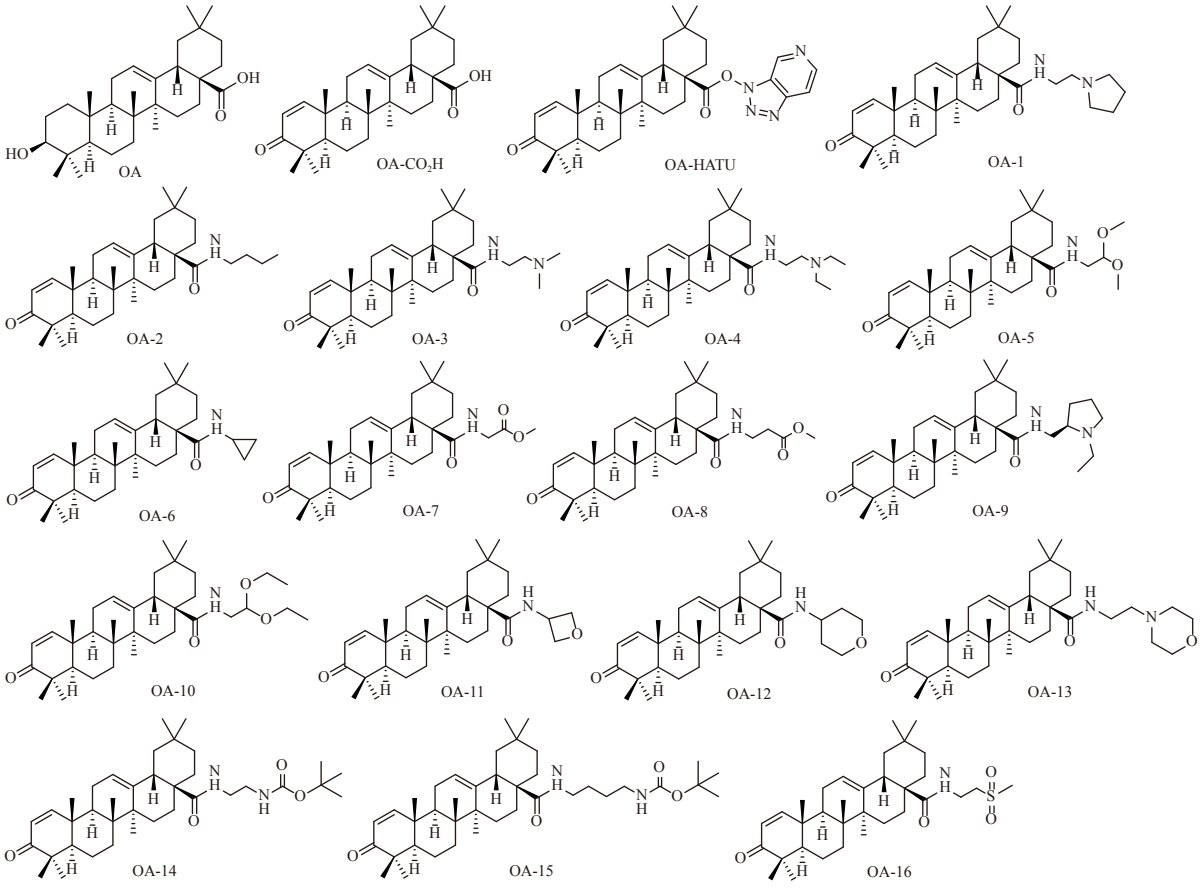

Fig. 1 The structures of oleanolic acid (OA) and its derivatives subjected to bioassay in this study

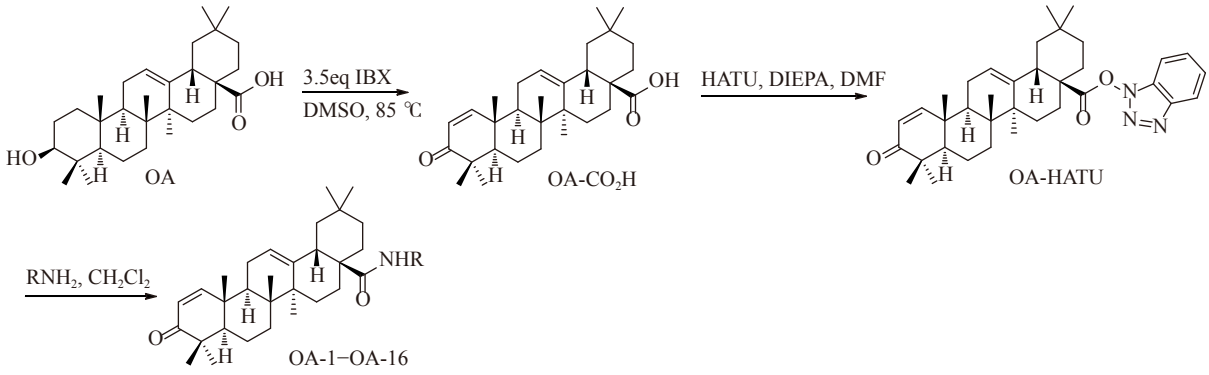

Fig. 2 Synthetic route for OA derivatives

against OA. First, the effects of all compounds on the viability of VEGF-stimulated HUVECs were assessed. As a result, all of OA derivatives, except OA-8, OA-9 and OA-12, were found to significantly inhibit the increased cell viability induced by VEGF at 10 μmol·L^{-1} (Fig. 3A), and most of these derivatives exhibited more potent activity compared with the parental OA. The preliminary structure-activity relationship (SAR) suggested that the introduction of *α*,*β*-unsaturated ketone system in Ring A of OA played an important role in anti-VEGF-induced proliferation, while the amide moiety at C-28 also affected their activity.

Furthermore, to determine the *in vitro* cytotoxicity of OA derivatives towards HUVECs, the cells were treated with these compounds at 10 μmol·L^{-1} for 24 h, and the cell viability was evaluated by SRB assay (Fig. 3B). The results showed that the compounds OA-CO_2H, OA-HATU, OA-2−OA-5, OA-9, OA-10, OA-13 and OA-14 exhibited undesired activity against the growth of HUVECs, while compounds OA-6, OA-7 and OA-11 increased the cell viability compared with the control group. Noticeably, compared with OA, two promising compounds OA-1 and OA-16 exhibited no obvious effects on normal cultured HUVECs but showed better inhibitory activity against VEGF-induced HUVECs with abnormally increased cell viability (Figs. 3A and 3B). Then EdU (5-ethynyl-2'-deoxyuridine) staining was performed, and the results from EdU staining also confirmed that OA-1 and OA-16 inhibited the proliferation of VEGF-induced HUVECs to the control level (Fig. 3C). Moreover, after treatment with the cells for 12 h, OA-1 and OA-16 showed better inhibitory effects on the proliferation induced by VEGF (Fig. S1). Based on these results, both compounds OA-1 and OA-16 were chosen as desirable hit compounds that would be tested for activity against VEGF-induced angiogenesis.

OA-1 and OA-16 inhibited VEGF-induced migration of HUVECs

To examine whether OA-1 and OA-16 inhibit VEGF-induced angiogenesis in HUVECs, an *in vitro* angiogenesis assay involving cell migration was performed. According to the results of wound healing assay, the wound width increased in response to VEGF. However, OA-1, OA-16, and OA effectively inhibited the migration of HUVECs induced by VEGF. Importantly, compared with OA, compounds OA-1 and OA-16 exhibited enhanced inhibitory activity against VEGF-induced HUVEC migration (Fig. 4).

OA-1 and OA-16 inhibited VEGF-induced tube formation of HUVECs

To further analyze the anti-angiogenic effects of OA-1 and OA-16, their activities towards tube formation of HUVECs were evaluated on the growth factor reduced Matrigel. When the cells were treated with VEGF, they became elongated and connected to each other to form a web-like structure after 3 h and 6 h (Fig. 5). However, after treatment with OA-1, OA-16 or OA, the VEGF-induced tube formation of HUVECs was effectively inhibited (Fig. 5). Moreover, compared with OA, derivatives OA-1 and OA-16 more significantly reduced VEGF-induced tube formation, indicating that OA-1 and OA-16 exhibited improved anti-angiogenic potential.

OA-1 and OA-16 inhibited VEGF-induced VEGFR2 activation in HUVECs

It has been reported that OA was an effective angiogenesis inhibitor by targeting VEGFR2 [26]. The VEGF/VEGF2 signaling is generally accepted as a key pathway leading to angiogenic responses in VECs. Many studies have shown that VEGFR2 binds to VEGF, activates several protein kinase pathways including the PI3K/AKT and ERK1/2 pathways and thus regulates cell proliferation, cell migration and tube formation [31-33]. Moreover, previous reports confirmed that OA inhibited VEGF2 activation by inhibiting VEGF-induced phosphorylation of VEGFR2 and its downstream signaling protein Erk1/2 [26]. Therefore, Western blot was performed to investigate whether OA-1 and OA-16 can also inhibit VEGFR2 activity in HUVECs. The cells were treated with VEGF (20 ng·mL^{-1}) for 6 h with or without OA-1 and OA-16 (10 μmol·L^{-1}). Compared with the VEGF-treated group, both OA-1 and OA-16 decreased the level of VEGF2, and inhibited the VEGF-induced phosphorylation of VEGFR2, Erk1/2 and AKT (Fig. 6). These results indicated that OA-1 and OA-16 effectively inhibited VEGF-induced VEGFR2 activation in HUVECs.

Knockdown of VEGFR2 abolished the inhibition effects of OA-1 and OA-16 on VEGF-induced angiogenesis

To further determine whether OA-1 and OA-16 inhib-

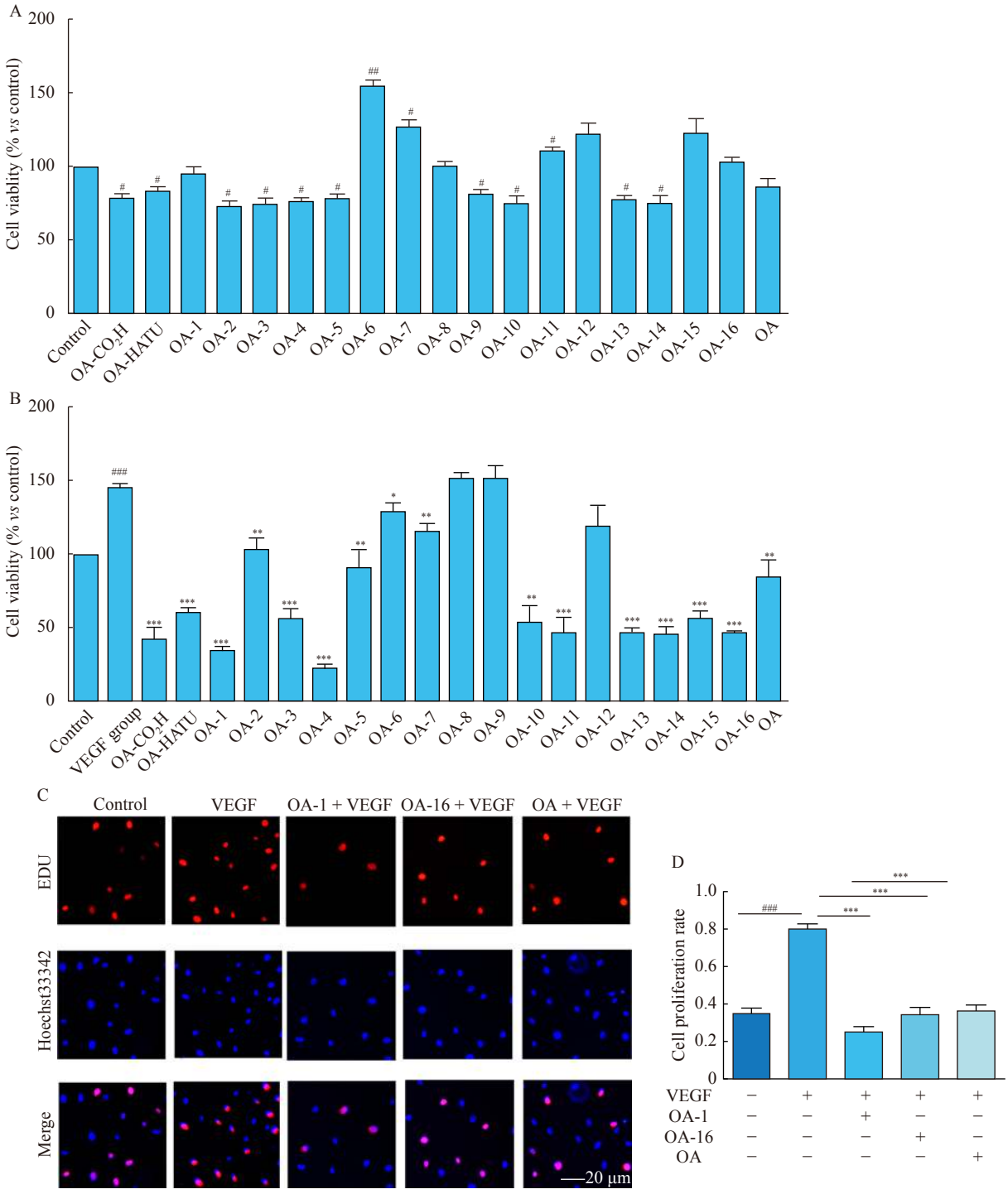

Fig. 3 Screening of OA derivatives that exhibit no effect on normal HUVECs but can inhibit abnormal proliferation of VEGF-induced endothelial cells. (A) HUVECs were treated with VEGF (20 ng·mL^{-1}) or VEGF and different OA derivatives (10 μmol·L^{-1}) for 24 h. The SRB assay was used to detect the effect of different OA derivatives on the increased cell viability induced by VEGF. (B) Effects of OA derivatives on the cell viability of HUVECs were detected by SRB assay after the cells were treated with different compounds for 24 h. (C) HUVECs were treated with VEGF (20 ng·mL^{-1}) or VEGF and OA-1, OA-16, and OA (10 μmol·L^{-1}) for 6 h, and cell proliferation was determined by EdU staining (200 ×). (D) Bar chart showing the HUVEC proliferation rate according to Hoechst 33342 and EdU staining. Data are presented as mean ± SEM (n = 3). $^{\#}P < 0.05$, $^{\#\#}P < 0.01$, and $^{\#\#\#}P < 0.001$ *vs* control, $^{*}P < 0.05$, $^{**}P < 0.01$, and $^{***}P < 0.001$ *vs* VEGF-treated group

ited VEGF2-induced angiogenesis *via* VEGFR2, VEGFR2 was knocked down by siRNA. As shown in Fig. 7, in the cells treated with non-silencing (scramble) small interfering RNA, OA-1 and OA16 effectively inhibited the migration

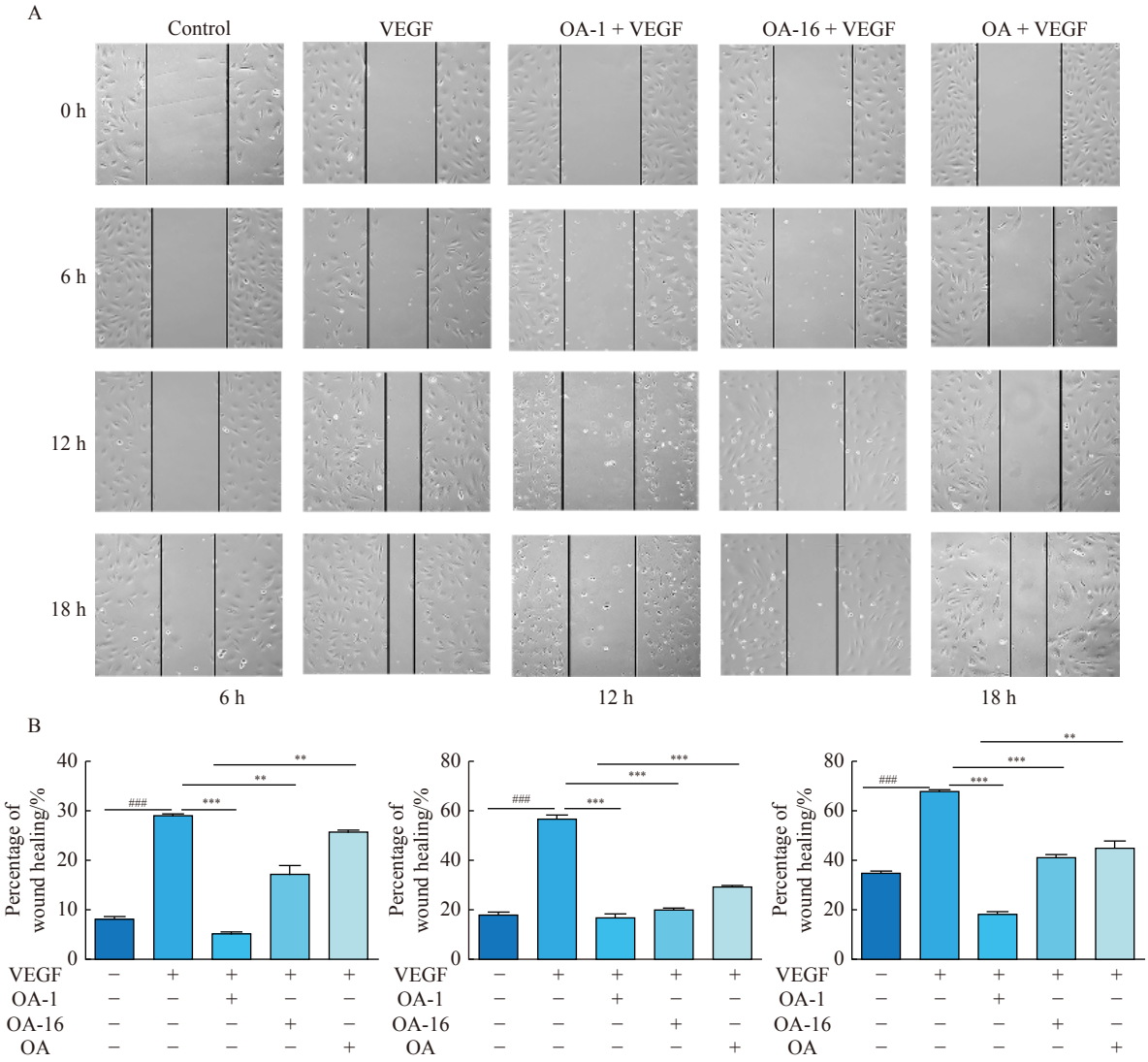

Fig. 4 Effects of OA-1, OA-16 and OA on VEGF-induced HUVEC migration. (A) Representative images of the migration of HUVECs treated with VEGF (20 mg·mL^{-1}), VEGF and OA-1, OA-16, or OA (10 μmol·L^{-1}). Original magnification was 100 ×. (B) Quantitative analysis of cell migration in panel (A). Data are presented as mean ± SEM (n = 3). $^{###}P < 0.001$ *vs* control, $^{**}P < 0.01$ and $^{***}P < 0.001$ *vs* VEGF-treated group

and tube formation of HUVECs induced by VEGF, whereas in the VEGFR2 knockdown cells, OA-1 or OA-16 exerted no significant effect on the migration and tube formation of HUVECs compared with VEGF-treated cells. Thus, these results indicated OA-1 and OA-16 inhibited angiogenesis through suppression of the VEGF/VEGFR2 signaling pathway.

Expermental

Reagents and equipment

Commercially available reagents were used without further purification. Organic solvents were evaporated under reduced pressure using a Büchi R-100 evaporator. Reactions were monitored by TLC using Yantai Jingyou (China) GF_{254} silica gel plates. Silica gel column chromatography was performed on silica gel (200−300 mesh) from Qingdao Hailang (China). NMR spectra were measured on a Bruker Avance III 600 MHz spectrometer. Chemical shifts were expressed in δ (ppm) and coupling constants (J) in Hz with solvent signals as internal standards ($CDCl_3$, δ_H 7.26 ppm and δ_C 77.2 ppm; and DMSO-d_6, δ_H 2.50 ppm and δ_C 39.5 ppm). HR-ESI-MS data were obtained on an Agilent Q-TOF 6520. The purity of the samples was determined by an analytical Shimadzu LC-20A HPLC with a SilGreen HPLC column GHO 525010C18A (10 mm × 250 mm) using parameters as follows: H_2O/MeOH, 10/90 to 0/100 in 20−30 min, plus 10 min isocratic MeOH at a flow rate of 3.0 mL·min^{-1}, λ = 210 nm and 254 nm.

Medium M199 and bovine serum were obtained from Gibco Co. (Carlsbad, CA, USA). Protein was extracted from cells using radio immunoprecipitation assay (RIPA) lysis buffer (Dingguo, Beijing, China). The primary antibodies anti-

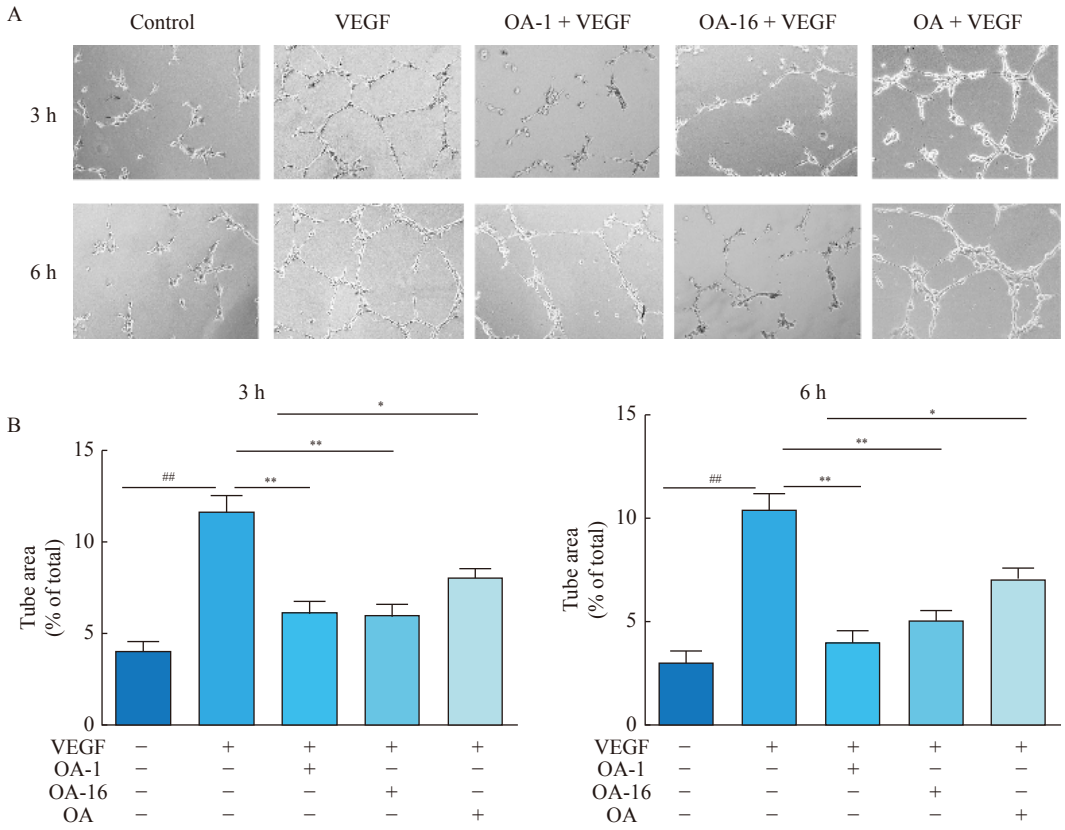

Fig. 5 Effects of OA-1, OA-16 and OA on VEGF-induced tube formation on Matrigel. (A) Representative images of tube formation of HUVECs treated with VEGF (20 ng·mL^{-1}), VEGF and OA-1, OA-16, or OA (10 μmol·L^{-1}). Original magnification was 100 ×. (B) Quantitative analysis of tube area in panel (A). Data are presented as mean ± SEM (n = 3). $^{\#\#}P < 0.01$ *vs* control, $^{*}P < 0.05$ and $^{**}P < 0.01$ *vs* VEGF-treated group

phospho-VEGFR-2, anti-VEGFR2, anti phospho-Erk1/2, anti-Erk, anti-AKT and anti phospho-AKT were obtained from Abclonal (Wuhan, China). The peroxidase-conjugated secondary antibodies were obtained from Abclonal (Wuhan, China).

Synthesis of OA-CO_2H

To a solvent of dimethyl sulfoxide (DMSO, 15 mL) in a round bottom flask were added OA (4.57 g, 10 mmol) and 2-iodoyl benzoic acid (IBX, 35 mmol). The mixture was stirred at 85 °C overnight. After completion of the reaction, the solution was diluted with ether (100 mL), washed twice with saturated $NaHCO_3$ solution and water. The organic phase was dried over anhydrous $MgSO_4$, then filtered and concentrated. The residue was purified by flash column chromatography (dichloromethane/methanol = 95/5) to obtain an OA-CO_2H white solid (2.9 g, yield 64.7 %). HPLC analysis: t_R = 14.03 min; peak area, > 95% (210 nm). mp: 258−260 °C. ^{1}H NMR (600 MHz, $CDCl_3$) δ: 7.02 (d, J = 10.1 Hz, 1H), 5.79 (d, J = 10.1 Hz, 1H), 5.33 (t, J = 3.7 Hz, 1H), 2.84 (dd, J = 13.9, 4.6 Hz, 1H), 2.15–1.09 (m, 28H), 1.06 (s, 3H), 0.92 (s, 3H), 0.90 (s, 3H), 0.83 (s, 3H). ^{13}C NMR (150 MHz, $CDCl_3$) δ: 159.2, 125.2, 122.0, 77.2, 53.5, 46.8, 45.8, 44.7, 42.1, 41.9, 41.3, 40.2, 39.6, 33.9, 33.2, 32.5, 32.5, 30.8, 27.9, 27.8, 26.0, 23.7, 23.4, 23.0, 21.7, 19.0, 18.8, 17.7. HR-ESI-MS: $[M + H]^+$ Calcd. for $C_{30}H_{45}O_3^+$ 453.3363, found 453.3365.

Synthesis of OA-HATU

To a solution of OA-CO_2H (2.72 g, 6 mmol, 1 eq) in 50 mL dichloromethane and 5 mL *N*,*N*-dimethylformamide was added HATU (2.51 g, 6.6 mmol, 1.1 eq). After the reaction was completed, the reaction solution was concentrated by evaporation under reduced pressure. The residue was diluted with ethyl acetate, and washed with water several times. Finally, the organic phase was dried over anhydrous $MgSO_4$, filtered and concentrated to yield a residue, which was subjected to flash column chromatography (dichloromethane/methanol = 95/5) to give OA-HATU (2.73 g, yield 79.7 %). HPLC analysis: t_R = 18.74 min; peak area, > 95% (254 nm). mp: 186−187 °C. ^{1}H NMR (600 MHz, $CDCl_3$) δ: 8.69 (dd, J = 4.5, 1.3 Hz, 1H), 8.39 (dd, J = 8.4, 1.3 Hz, 1H), 7.40 (dd, J = 8.4, 4.5 Hz, 1H), 7.02 (d, J = 10.2 Hz, 1H), 5.79 (d, J = 10.2 Hz, 1H), 5.41 (t, J = 3.7 Hz, 1H), 2.98 (dd, J = 13.8, 4.5 Hz, 1H), 2.30 (td, J = 13.8, 3.8 Hz, 1H), 1.85 (dd, J = 11.0, 6.4 Hz, 1H), 1.77 (t, J = 13.8 Hz, 1H), 1.43–1.36 (m, 2H), 1.15 (d, J = 8.5 Hz, 6H), 1.10 (s, 3H), 1.00–0.93 (m, 9H). ^{13}C NMR (150 MHz, $CDCl_3$) δ: 205.4, 173.5, 159.2, 151.7, 142.8, 141.0, 135.2, 129.4, 125.2, 123.2, 120.8, 53.6, 47.7, 45.5, 44.7, 42.4, 42.0, 41.9, 40.4, 39.5, 33.8, 33.1, 32.7, 32.2, 30.8, 28.2, 27.9, 25.8, 23.6, 23.5, 23.4, 21.8, 19.0, 18.8, 17.6.

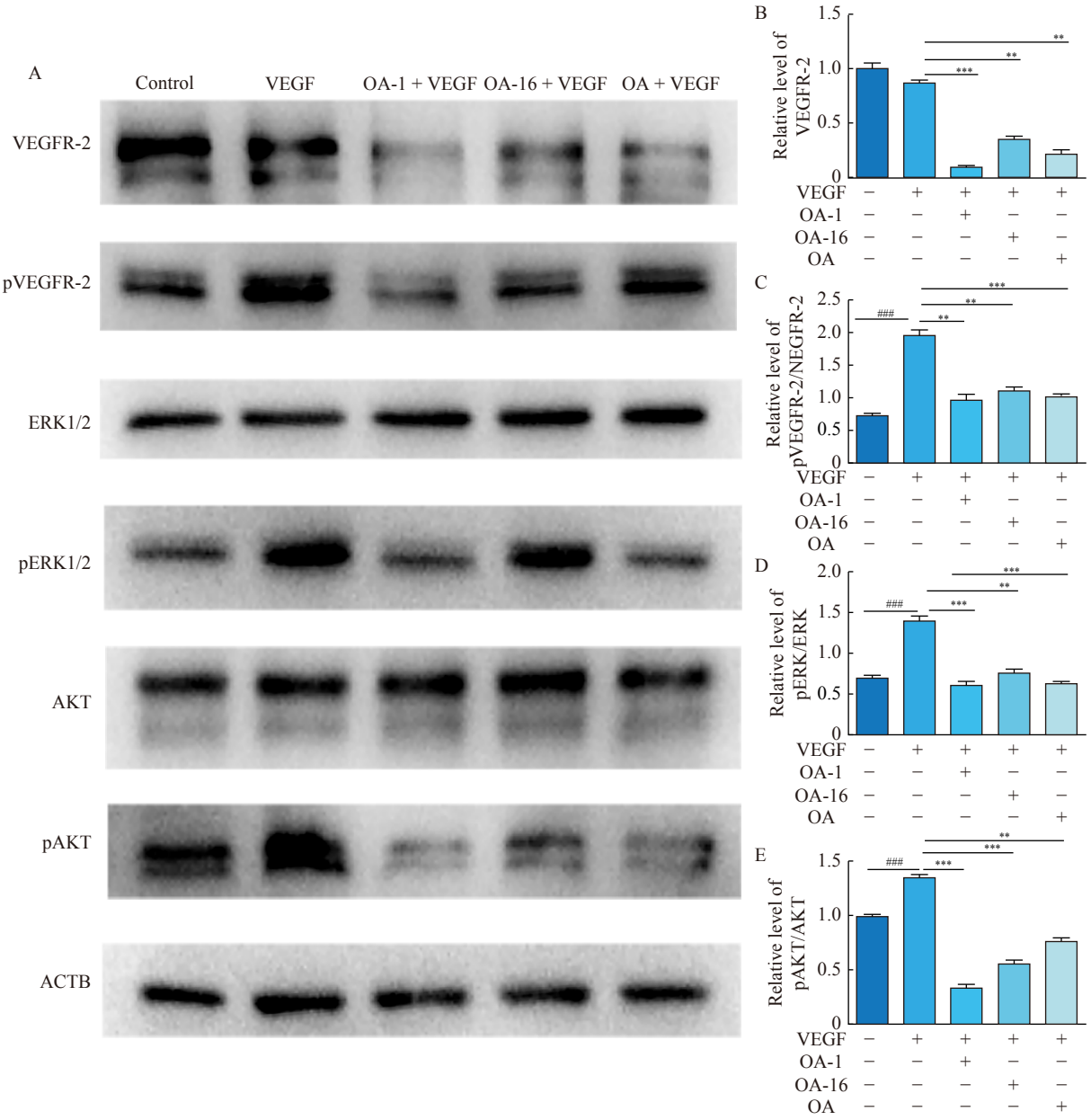

Fig. 6 Effects of OA-1 and OA-16 on VEGF-induced VEGFR2 activity. (A) HUVECs were treated with VEGF (20 ng·mL^{-1}), VEGF and OA-1, OA-16, or OA (10 μmol·L^{-1}) for 6 h. The phosphorylation of VEGFR2 (pVEGFR2), Erk1/2 (pErk1/2) and AKT (pAKT) was examined by Western blot analysis. (B) Quantification of VEGFR2 protein level in different groups. (C) Ratio of p-VEGFR2 to VEGFR2 in different group. (D) Relative level of p-ERK to total ERK in different groups. (E) Relative level of pAKT to total AKT in different groupss. Data are presented as mean ± SEM (n = 3). $^{\#\#\#}P < 0.001$ *vs* control, $^{**}P < 0.01$ and $^{***}P < 0.001$ *vs* VEGF-treated group

HR-ESI-MS: $[M + H]^+$ Calcd. for $C_{35}H_{47}N_4O_3^+$ 571.3643, found 571.3646.

General procedure for synthesis of OA-1−OA-16

To a solution of OA-HATU (114 mg, 0.2 mmol, 1 eq) in 5 mL dichloromethane were added the corresponding amines (1.1 eq) and DIPEA (142 μL, 0.8 mmol, 4 eq). The solution was stirred at room temperature overnight, and then extracted thrice using a mixed solution of dichloromethane (10 mL) with water (5 mL). The solution was dried over anhydrous $MgSO_4$, and then concentrated. The residue was subjected to flash column chromatography (dichloromethane/methanol = 95/5) as the eluent to obtain the target compounds.

OA-1: White solid, yield 67.2%. HPLC analysis: t_R = 9.37 min; peak area, > 95% (254 nm). mp: 72−74 °C. ^{1}H NMR (600 MHz, DMSO-d_6) δ: 7.15 (d, J = 10.2 Hz, 1H), 5.71 (d, J = 10.2 Hz, 1H), 5.28 (t, J = 3.7 Hz, 1H), 2.17 (dt, J = 18.0, 5.1 Hz, 1H), 1.75 (dd, J = 11.5, 6.0 Hz, 1H), 1.10 (d, J = 2.9 Hz, 6H), 1.05 (s, 3H), 0.99 (s, 3H), 0.87 (d, J = 5.7 Hz, 6H), 0.78 (s, 3H). ^{13}C NMR (150 MHz, DMSO-d_6) δ: 204.2, 176.7, 159.9, 144.8, 124.9, 121.6, 54.9, 54.0, 53.2,

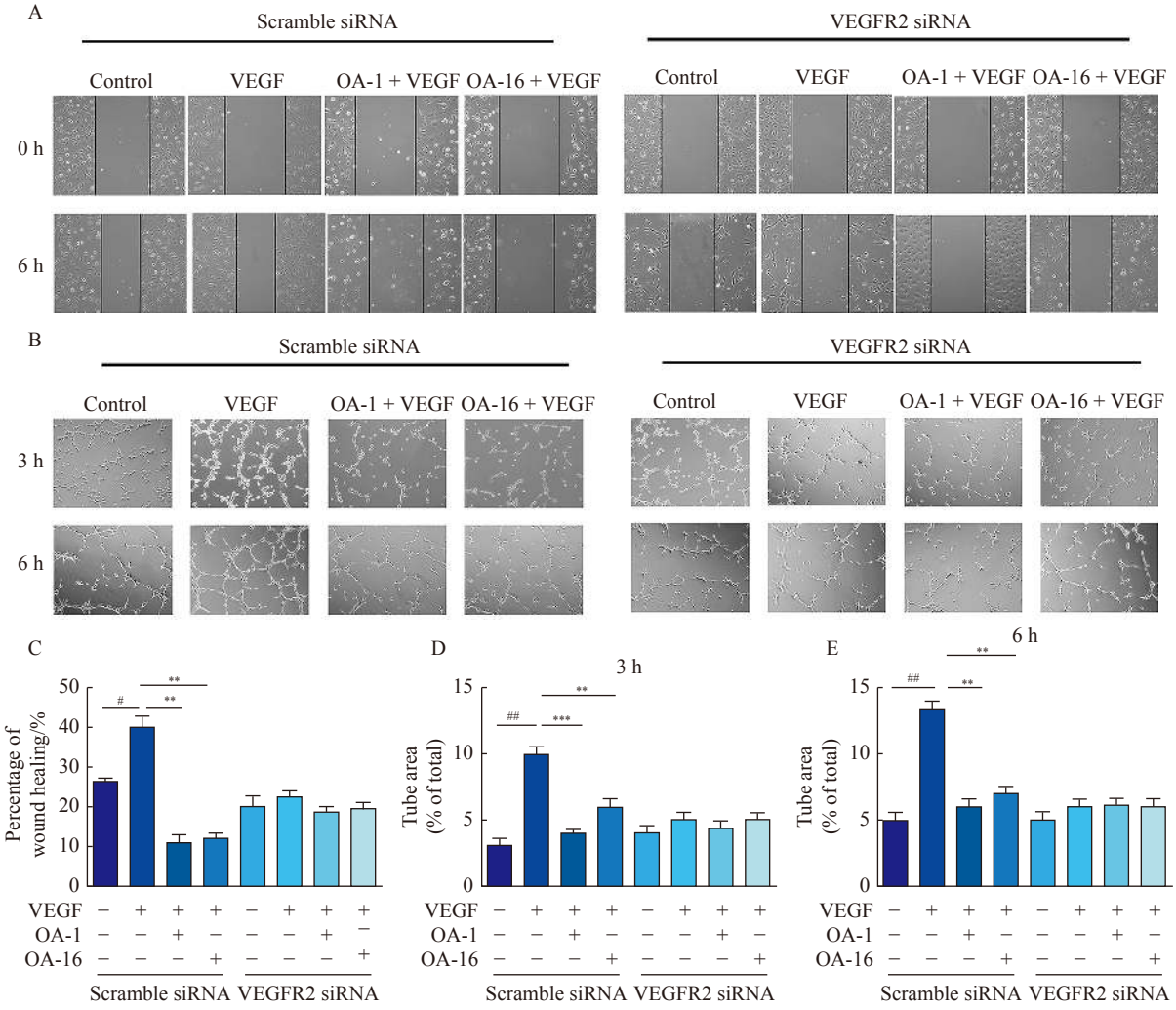

Fig. 7 Knockdown of VEGFR2 abolished the inhibitory effects of OA-1 and OA-16 on VEGF-induced migration and tube formation of HUVECs. HUVECs were treated with 40 nmol·L^{-1} VEGF2 siRNA or scramble siRNA for 24 h and stimulated with VEGF (20 ng·mL^{-1}), VEGF and OA-1 or OA-16 (10 μmol·L^{-1}) for indicated times. (A) Photomicrographs of HUVEC migration. (B) Photomicrographs of HUVEC on Matrigel. (C) Quantitative analysis of cell migration in panel (A). (D) and (E) Quantitative analysis of tube area in panel (B). Data are presented as mean ± SEM (n = 3). $^{\#\#}P < 0.01$ and $^{\#\#\#}P < 0.001$ *vs* control, $^{**}P < 0.01$ and $^{***}P < 0.001$ *vs* VEGF-treated group

46.3, 45.8, 44.3, 42.1, 41.7, 41.3, 38.7, 38.2, 34.1, 33.3, 33.0, 32.5, 30.9, 28.0, 27.3, 25.9, 23.9, 23.6, 23.2, 22.8, 21.8, 18.9, 17.6. HR-ESI-MS: $[M + H]^+$ Calcd. for $C_{36}H_{57}N_4O_2^+$ 549.4415, found 549.4415.

OA-2: White solid; yield 47.4%. HPLC analysis: t_R = 12.08 min; peak area, > 95% (254 nm). mp: 107−108 °C. ^{1}H NMR (600 MHz, $CDCl_3$) δ: 7.01 (d, J = 10.2 Hz, 1H), 5.90–5.83 (m, 1H), 5.80 (d, J = 10.2 Hz, 1H), 5.43 (t, J = 3.6 Hz, 1H), 3.39–3.31 (m, 1H), 3.04 (dtd, J = 13.4, 7.2, 4.6 Hz, 1H), 2.58–2.52 (m, 1H), 1.97 (td, J = 13.7, 3.8 Hz, 1H), 1.86 (dd, J = 11.3, 6.2 Hz, 1H), 1.76 (t, J = 13.4 Hz, 1H), 1.67 (d, J = 1.5 Hz, 2H), 1.45 (p, J = 7.3 Hz, 2H), 1.18–1.14 (m, 9H), 1.09 (s, 3H), 0.94 (s, 1H), 0.92 (s, 1H), 0.91 (d, J = 3.1 Hz, 6H), 0.86 (s, 3H). ^{13}C NMR (150 MHz, $CDCl_3$) δ: 205.3, 177.9, 158.8, 145.8, 125.3, 121.9, 53.5, 46.7, 46.5, 44.7, 42.6, 42.6, 41.9, 40.3, 39.5, 39.3, 34.3, 33.1, 32.7, 32.4, 31.6, 30.9, 27.9, 27.4, 25.8, 23.9, 23.7, 23.6, 21.8, 20.4, 19.0, 18.8, 17.5, 14.0. HR-ESI-MS: $[M + H]^+$ calcd for $C_{34}H_{54}NO_2^+$ 508.4149, found 508.4151.

OA-3: White solid; yield 69.2%. HPLC analysis: t_R = 12.46 min; peak area, > 95% (210 nm). mp: 112−113 °C. ^{1}H NMR (600 MHz, $CDCl_3$) δ: 7.01 (d, J = 10.2 Hz, 1H), 6.55 (t, J = 4.6 Hz, 1H), 5.79 (dd, J = 10.2, 1.4 Hz, 1H), 5.40 (t, J = 3.6 Hz, 1H), 3.39–3.31 (m, 1H), 3.17 (ddd, J = 11.4, 5.9, 2.9 Hz, 1H), 2.57 (dd, J = 13.3, 4.3 Hz, 1H), 2.41 (t, J = 6.0 Hz, 2H), 1.84 (dd, J = 11.4, 5.9 Hz, 1H), 1.17–1.13 (m, 10H), 1.08 (d, J = 1.5 Hz, 3H), 0.90 (d, J = 5.2 Hz, 6H), 0.87 (s, 3H). ^{13}C NMR (150 MHz, $CDCl_3$) δ: 205.3, 178.2, 158.9, 145.0, 125.3, 122.2, 57.8, 53.6, 53.4, 46.5, 46.5, 45.3, 44.7, 42.6, 42.5, 41.8, 40.3, 39.4, 36.9, 34.3, 33.1, 32.8, 32.4, 30.8, 27.9, 27.4, 25.7, 23.7, 23.7, 23.6, 21.7, 19.0, 18.8, 17.5. HR-ESI-MS: $[M + H]^+$ Calcd. for $C_{34}H_{55}N_2O_2^+$ 523.4258, found

523.4258.

OA-4: White solid; yield 49.9%. HPLC analysis: t_R = 14.08 min; peak area, > 95% (254 nm). mp: 121−122 °C. ^{1}H NMR (600 MHz, $CDCl_3$) δ: 7.01 (d, *J* = 10.2 Hz, 1H), 5.79 (d, *J* = 10.2 Hz, 1H), 5.41 (t, *J* = 3.7 Hz, 1H), 3.47 (dd, *J* = 13.7, 5.9 Hz, 1H), 3.12 (s, 1H), 1.96 (td, *J* = 13.7, 3.9 Hz, 1H), 1.85 (dd, *J* = 11.2, 6.4 Hz, 1H), 1.73 (t, *J* = 13.7 Hz, 1H), 1.38–1.32 (m, 2H), 1.17–1.12 (m, 10H), 1.07 (s, 9H), 0.90 (d, *J* = 4.5 Hz, 6H), 0.83 (s, 3H). ^{13}C NMR (150 MHz, $CDCl_3$) δ: 205.3, 177.9, 158.9, 145.1, 125.2, 122.0, 53.4, 51.7, 47.0, 46.6, 46.4, 44.7, 42.4, 42.2, 41.9, 40.2, 39.5, 36.5, 34.3, 33.2, 32.8, 32.3, 30.9, 27.9, 27.5, 25.9, 23.6, 23.5, 21.7, 19.0, 18.7, 17.4. HR-ESI-MS: $[M + H]^+$ Calcd. for $C_{36}H_{59}N_2O_2^+$ 551.4571, found 551.4570.

OA-5: White solid; yield 35.3%. HPLC analysis: t_R = 11.75 min; peak area, > 95% (254 nm). mp: 73−74 °C. ^{1}H NMR (600 MHz, $CDCl_3$) δ: 7.01 (d, *J* = 10.2 Hz, 1H), 6.12–6.06 (m, 1H), 5.80 (d, *J* = 10.2 Hz, 1H), 5.43 (t, *J* = 3.5 Hz, 1H), 4.37–4.32 (m, 1H), 3.53 (ddd, *J* = 13.7, 6.3, 4.7 Hz, 1H), 3.39 (d, *J* = 8.3 Hz, 6H), 3.18 (ddd, *J* = 13.7, 6.3, 4.7 Hz, 1H), 2.58 (dd, *J* = 13.2, 4.9 Hz, 1H), 1.18–1.14 (m, 9H), 1.09 (s, 3H), 0.91 (d, *J* = 2.2 Hz, 6H), 0.86 (s, 3H). ^{13}C NMR (150 MHz, $CDCl_3$) δ: 205.3, 178.2, 158.8, 145.2, 125.3, 122.2, 103.0, 54.7, 54.6, 53.5, 46.6, 46.5, 44.7, 42.5, 42.5, 41.8, 41.2, 40.3, 39.5, 34.2, 33.1, 32.8, 32.4, 30.9, 27.9, 27.4, 25.8, 23.8, 23.7, 23.6, 21.8, 19.0, 18.8, 17.5. HR-ESI-MS: $[M + H]^+$ Calcd. for $C_{34}H_{54}NO_4^+$ 540.4047, found 540.4048.

OA-6: White solid; yield 64.2%. HPLC analysis: t_R = 11.07 min; peak area, > 95% (254 nm). mp: 132−133 °C. ^{1}H NMR (600 MHz, $CDCl_3$) δ: 7.01 (d, *J* = 9.4 Hz, 1H), 5.96 (s, 1H), 5.80 (d, *J* = 9.4 Hz, 1H), 5.40 (s, 1H), 2.64 (d, *J* = 3.7 Hz, 1H), 2.54–2.46 (m, 1H), 1.97 (td, *J* = 13.7, 3.7 Hz, 1H), 1.55 (t, *J* = 12.9 Hz, 6H), 1.20–1.09 (m, 15H), 0.94–0.85 (m, 9H), 0.50–0.34 (m, 2H). ^{13}C NMR (150 MHz, $CDCl_3$) δ: 205.2, 179.4, 158.7, 145.5, 125.2, 121.9, 53.3, 46.5, 46.1, 44.5, 42.4, 42.4, 41.7, 40.2, 39.4, 34.1, 33.0, 32.4, 32.2, 30.7, 27.8, 27.2, 25.6, 23.7, 23.6, 23.4, 22.6, 21.6, 18.8, 18.7, 17.4, 6.7, 6.1. HR-ESI-MS: $[M + H]^+$ Calcd. for $C_{33}H_{50}NO_2^+$ 492.3836, found 492.3837.

OA-7: White solid; yield 44.7%. HPLC analysis: t_R = 9.81 min; peak area, > 95% (254 nm). mp: 113−115 °C. ^{1}H NMR (600 MHz, $CDCl_3$) δ: 7.02 (d, *J* = 10.2 Hz, 1H), 6.54–6.45 (m, 1H), 5.80 (d, *J* = 10.2 Hz, 1H), 5.52 (t, *J* = 3.7 Hz, 1H), 4.12 (dd, *J* = 18.7, 5.5 Hz, 1H), 3.86 (dd, *J* = 18.7, 3.7 Hz, 1H), 3.76 (s, 3H), 2.70–2.64 (m, 1H), 2.02 (td, *J* = 13.6, 4.0 Hz, 1H), 1.86 (dd, *J* = 10.9, 6.6 Hz, 1H), 1.77 (t, *J* = 13.6 Hz, 1H), 0.92 (d, *J* = 6.6 Hz, 6H), 0.80 (s, 3H). ^{13}C NMR (150 MHz, $CDCl_3$) δ: 205.3, 178.2, 170.7, 158.9, 145.0, 125.3, 122.6, 53.5, 52.5, 46.5, 44.7, 42.4, 41.9, 41.7, 40.3, 39.5, 34.2, 33.1, 32.5, 32.3, 30.9, 27.9, 27.4, 25.8, 23.9, 23.7, 23.6, 21.8, 19.0, 18.8, 17.1, 1.2. HR-ESI-MS: $[M + H]^+$ Calcd. for $C_{33}H_{50}NO_4^+$ 524.3734, found 524.3734.

OA-8: White solid; yield 71.5%. HPLC analysis: t_R = 10.41 min; peak area, > 95% (254 nm). mp: 96−97 °C. ^{1}H NMR (600 MHz, $CDCl_3$) δ: 7.01 (d, *J* = 10.2 Hz, 1H), 6.46 (t, *J* = 6.0 Hz, 1H), 5.80 (d, *J* = 10.2 Hz, 1H), 5.43 (t, *J* = 3.6 Hz, 1H), 3.70 (s, 3H), 3.58 (dd, *J* = 12.9, 6.0 Hz, 1H), 3.40 (dd, *J* = 13.3, 7.7 Hz, 1H), 2.56 (dt, *J* = 13.3, 3.1 Hz, 1H), 2.51 (dt, *J* = 6.4, 5.0 Hz, 2H), 2.14 (dd, *J* = 6.4, 4.2 Hz, 1H), 2.10 (dd, *J* = 11.3, 3.1 Hz, 1H), 1.97 (td, *J* = 13.7, 3.9 Hz, 1H), 1.87–1.83 (m, 1H), 1.17–1.13 (m, 9H), 1.08 (s, 3H), 0.90 (d, *J* = 2.4 Hz, 6H), 0.8 (s, 3H). ^{13}C NMR (150 MHz, $CDCl_3$) δ: 205.3, 178.0, 173.4, 158.9, 144.9, 125.3, 122.3, 53.4, 51.9, 46.6, 44.7, 42.5, 42.4, 41.8, 40.3, 39.5, 34.8, 34.2, 33.9, 33.1, 32.9, 32.4, 30.9, 27.9, 27.4, 25.8, 23.7, 23.7, 23.5, 21.8, 19.0, 18.8, 17.5. HR-ESI-MS: $[M + H]^+$ Calcd. for $C_{35}H_{54}NO_3^+$ 536.4098, found 538.4098.

OA-9: White solid; yield 37.7%. HPLC analysis: t_R = 11.50 min; peak area, > 95% (254 nm). mp: 116−117 °C. ^{1}H NMR (600 MHz, $CDCl_3$) δ: 7.01 (d, *J* = 10.2 Hz, 1H), 6.14 (dd, *J* = 7.0, 4.3 Hz, 1H), 5.80 (d, *J* = 10.2 Hz, 1H), 5.42 (t, *J* = 3.6 Hz, 1H), 4.46 (dd, *J* = 6.7, 4.6 Hz, 1H), 3.71 (ddd, *J* = 14.9, 9.4, 7.1 Hz, 2H), 3.61 (ddd, *J* = 13.7, 6.6, 4.6 Hz, 1H), 3.53 (ddd, *J* = 9.4, 7.9, 7.1 Hz, 2H), 3.09 (ddd, *J* = 13.7, 6.6, 4.2 Hz, 1H). ^{13}C NMR (150 MHz, $CDCl_3$) δ: 205.2, 178.0, 158.7, 145.2, 125.2, 122.0, 100.9, 63.0, 62.9, 53.3, 46.5, 46.4, 44.6, 42.4, 42.3, 42.0, 41.7, 40.1, 39.4, 34.1, 33.0, 32.6, 32.2, 30.7, 27.7, 27.3, 25.7, 23.7, 23.5, 23.4, 21.6, 18.9, 18.6, 17.3, 15.4, 15.4. HR-ESI-MS: $[M + H]^+$ Calcd. for $C_{37}H_{59}N_2O_2^+$ 563.4571, found 563.4575.

OA-10: White solid; yield 66.3%. HPLC analysis: t_R = 17.94 min; peak area, > 95% (254 nm). mp: 85−86 °C. ^{1}H NMR (600 MHz, $CDCl_3$) δ: 7.01 (dd, *J* = 10.2, 3.1 Hz, 1H), 6.55 (s, 1H), 5.80 (dd, *J* = 10.2, 2.0 Hz, 1H), 5.40 (t, *J* = 3.6 Hz, 1H), 0.93–0.89 (m, 6H), 0.84 (d, *J* = 5.1 Hz, 3H). ^{13}C NMR (150 MHz, $CDCl_3$) δ: 205.2, 178.1, 158.8, 158.6, 145.2, 125.1, 125.0, 121.6, 53.4, 53.3, 53.3, 46.5, 46.4, 46.2, 44.5, 42.2, 41.7, 40.1, 39.8, 39.3, 33.0, 32.9, 32.1, 30.7, 27.9, 27.7, 27.7, 27.3, 27.3, 25.6, 25.6, 23.5, 23.4, 23.3, 21.6, 18.8, 18.6, 18.6, 17.1. HR-ESI-MS: $[M + H]^+$ Calcd. for $C_{23}H_{25}N_5O^+$ 568.4360, found 568.4365.

OA-11: White solid; yield 28.7%. HPLC analysis: t_R = 12.05 min; peak area, > 95% (254 nm). mp: 128−130 °C. ^{1}H NMR (600 MHz, $CDCl_3$) δ: 7.01 (d, *J* = 10.2 Hz, 1H), 6.32 (d, *J* = 5.9 Hz, 1H), 5.81 (d, *J* = 10.2 Hz, 1H), 5.49 (t, *J* = 3.6 Hz, 1H), 5.29 (s, 1H), 4.93 (dq, *J* = 13.7, 6.8 Hz, 2H), 4.87 (t, *J* = 6.8 Hz, 1H), 4.45 (t, *J* = 5.5 Hz, 2H), 2.62 (d, *J* = 13.2 Hz, 1H), 2.22–2.06 (m, 3H), 2.01 (td, *J* = 13.7, 13.2, 3.4 Hz, 2H), 1.87 (dd, *J* = 11.3, 6.2 Hz, 1H), 1.77 (t, *J* = 13.4 Hz, 2H), 1.65 (ddd, *J* = 13.4, 8.9, 4.7 Hz, 4H), 1.56 (m, 8H), 1.36 (dp, *J* = 13.6, 5.2, 4.4 Hz, 4H), 1.24–1.15 (m, 16H), 1.09 (s, 3H), 0.92 (d, J = 4.8 Hz, 7H), 0.85 (s, 3H). ^{13}C NMR (150 MHz, $CDCl_3$) δ: 205.2, 178.0, 158.7, 145.5, 125.4, 122.3, 78.9, 78.0, 53.4, 46.5, 46.4, 45.1, 44.7, 42.6, 42.5, 41.8, 40.3, 39.5, 34.2, 33.1, 32.7, 32.4, 30.9, 27.9, 27.4, 25.8, 23.9, 23.7, 23.6, 21.8, 18.9, 18.8, 17.6. HR-ESI-MS: $[M + H]^+$ Calcd. for $C_{33}H_{50}NO_3^+$ 508.3791, found 508.3793.

OA-12: White solid; yield 22.8%. HPLC analysis: t_R =

13.30 min; peak area, > 95% (254 nm). mp: 131−133 °C. ^{1}H NMR (600 MHz, $CDCl_3$) δ: 7.01 (d, *J* = 10.2 Hz, 1H), 5.80 (d, *J* = 10.2 Hz, 1H), 5.68 (d, *J* = 7.3 Hz, 1H), 5.42 (t, *J* = 3.6 Hz, 1H), 3.94 (tdd, *J* = 11.8, 5.8, 2.4 Hz, 3H), 3.46 (tdd, *J* = 11.8, 5.8, 2.4 Hz, 2H), 2.61–2.55 (m, 1H), 1.92–1.82 (m, 3H), 1.76 (t, *J* = 13.4 Hz, 1H), 0.93–0.88 (m, 9H). ^{13}C NMR (150 MHz, $CDCl_3$) δ: 205.1, 177.1, 158.6, 145.2, 125.1, 121.8, 66.8, 66.7, 53.2, 46.4, 46.2, 45.6, 44.5, 42.5, 42.3, 41.6, 40.1, 39.3, 34.0, 33.2, 32.9, 32.9, 32.7, 32.3, 30.6, 27.7, 27.2, 25.5, 23.6, 23.5, 23.4, 21.6, 18.8, 18.6, 18.0. HR-ESI-MS: $[M + H]^+$ Calcd. for $C_{35}H_{54}NO_3^+$ 536.4104, found 536.4107.

OA-13: White solid; yield 34.7%. HPLC analysis: t_R = 11.15 min; peak area, > 95% (254 nm). mp: 183−184 °C. ^{1}H NMR (600 MHz, $CDCl_3$) δ: 7.01 (d, *J* = 10.2 Hz, 1H), 6.47 (t, *J* = 4.6 Hz, 1H), 5.81 (d, *J* = 10.2 Hz, 1H), 5.43 (t, *J* = 3.6 Hz, 1H), 3.77–3.67 (m, 4H), 3.46–3.39 (m, 1H), 3.24–3.16 (m, 1H), 2.59–2.53 (m, 1H), 2.50–2.40 (m, 6H), 2.18 (ddd, *J* = 18.1, 6.2, 4.3 Hz, 1H), 2.07 (ddd, *J* = 18.1, 11.4, 3.1 Hz, 1H), 1.97 (td, *J* = 13.5, 3.8 Hz, 1H), 1.88 (dd, *J* = 11.4, 6.2 Hz, 1H), 1.76 (t, *J* = 13.5 Hz, 1H), 1.72–1.65 (m, 2H), 1.38–1.32 (m, 2H), 1.14 (d, *J* = 2.8 Hz, 6H), 1.08 (s, 3H), 0.91 (s, 6H), 0.85 (s, 3H). ^{13}C NMR (150 MHz, $CDCl_3$) δ: 205.3, 177.9, 158.7, 145.5, 125.4, 121.8, 67.2, 57.0, 53.5, 53.4, 46.7, 46.6, 44.7, 42.6, 42.5, 41.8, 40.3, 39.5, 35.6, 34.3, 33.1, 32.8, 32.3, 30.9, 27.9, 27.4, 25.8, 23.8, 23.6, 23.6, 21.8, 19.0, 18.8, 17.5. HR-ESIS: $[M + H]^+$ Calcd. for $C_{36}H_{57}N_2O_3^+$ 565.4369, found 565.4373.

OA-14: White solid; yield 44.8%. HPLC analysis: t_R = 29.23 min; peak area, > 95% (254 nm). mp: 193−195 °C. ^{1}H NMR (600 MHz, $CDCl_3$) δ: 8.69 (d, *J* = 4.5 Hz, 1H), 8.39 (d, *J* = 8.3 Hz, 1H), 7.41 (dd, *J* = 8.3, 4.5 Hz, 1H), 7.02 (d, *J* = 10.2 Hz, 1H), 5.80 (d, *J* = 10.2 Hz, 1H), 5.41 (t, *J* = 3.8 Hz, 1H), 2.98 (dd, *J* = 13.8, 4.8 Hz, 1H), 1.82 (t, *J* = 13.8 Hz, 1H). ^{13}C NMR (150 MHz, $CDCl_3$) δ: 205.4, 173.5, 159.2, 151.7, 142.8, 141.0, 135.2, 129.4, 125.2, 123.2, 120.8, 53.6, 47.7, 45.5, 44.7, 42.4, 42.0, 41.9, 40.4, 39.6, 33.8, 33.1, 32.7, 32.2, 30.8, 28.2, 27.9, 25.8, 23.7, 23.5, 23.4, 21.8, 19.1, 18.9, 17.6. HR-ESI-MS: $[M + H]^+$ Calcd. for $C_{37}H_{59}N_2O_4^+$ 595.4475, found 595.4480.

OA-15: White solid; yield 87.4%. HPLC analysis: t_R = 20.41 min; peak area, > 95% (254 nm). mp: 120−121 °C. ^{1}H NMR (600 MHz, $CDCl_3$) δ: 7.01 (d, *J* = 10.2 Hz, 1H), 5.96 (t, *J* = 5.5 Hz, 1H), 5.80 (d, *J* = 10.2 Hz, 1H), 5.44 (d, *J* = 3.5 Hz, 1H), 4.68–4.55 (m, 1H), 3.37 (dq, *J* = 13.1, 6.5 Hz, 1H), 3.12 (d, *J* = 6.5 Hz, 2H), 2.57 (dd, *J* = 13.1, 4.3 Hz, 1H), 1.43 (s, 9H), 1.18–1.13 (m, 9H), 1.08 (s, 3H). ^{13}C NMR (150 MHz, $CDCl_3$) δ: 205.3, 178.1, 158.8, 156.1, 145.7, 125.3, 122.0, 53.4, 46.7, 46.5, 44.7, 42.5, 42.5, 41.8, 40.3, 39.5, 39.3, 34.2, 33.1, 32.8, 32.3, 30.9, 28.5, 27.9, 27.8, 27.4, 26.9, 25.8, 23.8, 23.7, 23.6, 21.7, 19.0, 18.8, 17.5. HR-ESI-MS: $[M + H]^+$ Calcd. for $C_{39}H_{63}N_2O_4^+$ 623.4788, found 623.4788.

OA-16: White solid; yield 71.6%. HPLC analysis: t_R = 12.66 min; peak area, > 95% (254 nm). mp: 114−115 °C. ^{1}H NMR (600 MHz, $CDCl_3$) δ: 7.01 (d, *J* = 10.2 Hz, 1H), 6.60 (t, *J* = 5.8 Hz, 1H), 5.80 (d, *J* = 10.2 Hz, 1H), 5.45 (t, *J* = 3.7 Hz, 1H), 3.89 (dtd, *J* = 14.7, 6.4, 4.8 Hz, 1H), 3.58 (ddt, *J* = 14.7, 8.2, 4.8 Hz, 1H), 3.25 (ddd, *J* = 13.4, 8.2, 4.8 Hz, 1H), 3.17 (ddd, *J* = 14.2, 6.4, 4.8 Hz, 1H), 2.95 (s, 3H), 2.63–2.57 (m, 1H), 2.00 (dd, *J* = 13.7, 4.0 Hz, 1H), 1.85 (dd, *J* = 10.8, 6.7 Hz, 1H), 0.91 (d, *J* = 4.5 Hz, 6H). ^{13}C NMR (150 MHz, $CDCl_3$) δ: 205.3, 178.6, 158.8, 144.5, 125.3, 122.8, 54.0, 53.4, 46.6, 46.5, 44.7, 42.4, 42.1, 41.8, 41.6, 40.3, 39.5, 34.2, 33.2, 33.1, 32.7, 32.3, 30.8, 27.8, 27.4, 25.9, 23.7, 23.6, 23.5, 21.8, 19.0, 18.8, 17.5. HR-ESI-MS: $[M + H]^+$ Calcd. for $C_{33}H_{52}NO_4S^+$ 558.3617, found 558.3616.

Cell culture

Human umbilical vascular endothelial cells (HUVECs) were obtained from ScienCell (San Diego, CA, USA) and cultured on gelatin-coated plastic dishes in M199 medium with 20% (*V*/*V*) bovine serum and 10 IU·mL^{-1} fibroblast growth factor 2 (FGF2). The cells were maintained at 37 °C under humidified conditions and 5% CO_2. Cells at not more than passage 10 were used for experiments.

Cell viability assay

HUVECs were seeded into 96-well plates and treated with oleanolic acid or different derivatives for 24 h. After fixing with trichloroacetic acid, the cells were stained with 0.4% (*W*/*V*) sulforhodamine B (SRB) dissolved in 1% acetic acid for 30 min. Then, the cells were rinsed with 1% acetic acid for 5 times. 96-well plates were dried at room temperature, 100 μL of 10 mmol·L^{-1} Trisbase (pH 10.5) was added and oscillated for 5 min. The absorbance was detected at 540 nm wavelength using a microplate spectrophotometer (TECAN, USA).

Cell proliferation

Cell proliferation was determined by EdU (5-ethynyl-2'-deoxyuridine) staining. Briefly, HUVECs were seeded into 24-well plates at 10^4 cells/mL and incubated overnight, before treatment with VEGF (20 ng·mL^{-1}) and oleanolic acid or related derivatives (10 μmol·L^{-1}) for 6 h. The cells were fixed in 4% formaldehyde for 30 min, then incubated with Hoechst 33342 (2 mg·mL^{-1}) and 50 μmol·L^{-1} Edu at 37 °C for 30 min. Stained cells were washed with PBS and then observed under an inverted fluorescence microscope (Olympus, Japan).

Matrigel assay

The 24-well culture plates were coated with growth factor reduced matrigel (BD, USA) according to the manufacturer's instructions. HUVECs were seeded at 5 × 10^4 cells/well, followed by VEGF (20 ng·mL^{-1}) and different oleanolic acid derivatives treatment for 3 h or 6 h. Tubule formation images were captured at a magnification of 100 × with a digital microscope camera system (Olympus, Japan).

Cell migration assay

Cell migration was determined by wound healing assay. Briefly, HUVECs were seeded in 6 cm dishes at 10^4 cells/mL. When the cells reached a post-confluent state, wounds of 1 mm width were created by scraping cell monolayers with a sterile pipette tip. Then, the cells were treated with VEGF (20 ng·mL^{-1}) and oleanolic acid or related deriv-

atives (10 μmol·L^{-1}) for 6 h, 12 h or 18 h, respectively and photographs were captured under a light microscope (Olympus, Japan). Cell migration was quantified by measuring the distance between the wound edges by Image J software.

Western blot analysis

Protein was extracted from cells using radio immunoprecipitation assay (RIPA) lysis buffer (Dingguo, Beijing, China) containing proteinase inhibitors (Sigma-Aldrich, USA). The lysate was centrifuged at 12 000 r·min^{-1} at 4 °C for 15 min. The supernatant was then collected and the protein concentration was determined using BCA Protein Assay kit (Beyotime, China). Equal amounts of protein lysates (15 μg per lane) were separated on 15% SDS-PAGE gels and transferred onto PVDF membrane (Millipore, Madison, WI, USA). The membrane was blocked with 5% non-fat dry milk in Tris-buffered saline containing 0.1% Tween-20 (TBST) for 2 h to reduce non-specific binding. The membrane was incubated with primary antibodies at 4 °C overnight. After washing with TBST three times, the membrane was incubated with HRP-conjugated secondary antibody (Dingguo, Beijing, China) at room temperature for 1.5 h. Immune complexes were detected by enhanced chemiluminescence (Millipore Corporation, Billerica, USA). Integrated densities of bands were quantified by Image J software.

RNA interference experiments

HUVECs were transfected with scramble RNA (negative control) or siRNA against VEGFR2 (40 mol·L^{-1}) for 24 h by use of Lipo2000 transfection reagent (Invitrogen, USA) according to the manufacturer's instructions. The efficiency of RNA interference was determined by Western blot.

Statistical analysis

Data are presented as mean ± SEM. Images were processed by GraphPad Prism 5 (GraphPad Software, La Jolla, CA, USA) and Adobe Photoshop (Adobe, San Jose, USA). At least three independent replications were performed. One-way ANOVA combined with Bonferroni post hoc tests were used to determine the significance between different groups. $P < 0.05$ was considered statistically significant.

Conclusions

The present study was aimed to improve the inhibitory activity of OA against VEGF and VEGF-induced angiogenesis by structural modification. Resutls showed that 16 target OA derivatives were prepared through introduction of *α*,*β*-unsaturated ketone system in ring A and amide functional group at C-28 of OA. The bioassay results indicated that some of OA derivatives showed promising inhibitory activity against VEGF-induced proliferation in HUVECs. Among them, two desirable derivatives OA-1 and OA-16 exhibited more potent activity than OA in inhibiting the abnormal proliferation and angiogenesis of HUVECs induced by VEGF, but had no significant cytotoxicity towards normal HUVECs. Furthermore, compounds OA-1 and OA-16 were shown to decrease the expression of VEGFR2 and also inhibit the VEGF-induced phosphorylation of VEGFR2 and its downstream signaling protein Erk1/2 and AKT. Small interfering RNA experiments were performed and confirmed that OA-1 and OA-16 inhibited VEGF-induced angiogenesis *via* VEGFR2. The preliminary SAR study suggested that the *α*,*β*-unsaturated ketone system in ring A and amide side chain at C-28 played an important role in the activity of OA derivatives. Overall, the present research work demonstrated these OA derivatives as new potent VEGF-targeted angiogenesis inhibitors, and further structural optimization towards this series of compounds may provide lead compounds for the discovery of anti-angiogenesis-related drugs.

Supplementary Material

Supplementray information can be acquired by e-mail to corresponding author.

References

[1] MacDonald IJ, Liu SC, Su DM, *et al*. Implications of angiogenesis involvement in arthritis [J]. *Int J Mol Sci*, 2018, **19**(7): 2012.

[2] Liu GH, Chen T, Ding ZY, *et al*. Inhibition of FGF-FGFR and VEGF-VEGFR signalling in cancer treatment [J]. *Cell Prolif*, 2021, **54**(4): e13009.

[3] Mousa SA, Mousa SS. Current status of vascular endothelial growth factor inhibition in age-related macular degeneration [J]. *BioDrugs*, 2010, **24**(3): 183-194.

[4] Apte RS, Chen DS, Ferrara N. VEGF in signaling and disease: Beyond discovery and development [J]. *Cell*, 2019, **176**(6): 1248-1264.

[5] Mochizuki M, Güç E, Park AJ, *et al*. Growth factors with enhanced syndecan binding generate tonic signalling and promote tissue healing [J]. *Nat Biomed Eng*, 2020, **4**(4): 463-475.

[6] Yu PC, Wilhelm K, Dubrac A, *et al*. FGF-dependent metabolic control of vascular development [J]. *Nature*, 2017, **545**(7653): 224-228.

[7] Leung DW, Cachianes G, Kuang WJ, *et al*. Vascular endothelial growth factor is a secreted angiogenic mitogen [J]. *Science*, 1989, **246**(4935): 1306-1309.

[8] Ranieri G, Patruno R, Ruggieri E, *et al*. Vascular endothelial growth factor (VEGF) as a target of bevacizumab in cancer: From the biology to the clinic [J]. *Curr Med Chem*, 2006, **13**(16): 1845-1857.

[9] Chuai YH, Rizzuto I, Zhang X, *et al*. Vascular endothelial growth factor (VEGF) targeting therapy for persistent, recurrent, or metastatic cervical cancer [J]. *Cochrane Database Syst Rev*, 2021, **3**: CD013348.

[10] Lee TK, Park JY, Yu JS, *et al*. 7*α*,15-Dihydroxydehydroabietic acid from *Pinus koraiensis* inhibits the promotion of angiogenesis through downregulation of VEGF, p-Akt and p-ERK in HUVECs [J]. *Bioorg Med Chem Lett*, 2018, **28**(6): 1084-1089.

[11] Tajima H, Honda T, Kawashima K, *et al*. Pyridylmethylthio derivatives as VEGF inhibitors. Part 1 [J]. *Bioorg Med Chem Lett*, 2010, **20**(24): 7234-7238.

[12] Fukumura D, Kloepper J, Amoozgar Z, *et al*. Enhancing cancer immunotherapy using antiangiogenics: opportunities and challenges [J]. *Nat Rev Clin Oncol*, 2018, **15**(5): 325-340.

[13] Mei J, Tian HX, Huang HS, *et al*. Cellular models of development of ovarian high-grade serous carcinoma: A review of cell of origin and mechanisms of carcinogenesis [J]. *Cell Prolif*, 2021, **54**(5): e13029.

[14] Pandey AK, Singhi EK, Arroyo JP, *et al*. Mechanisms of VE-

GF (vascular endothelial growth factor) inhibitor–associated hypertension and vascular disease [J]. *Hypertension*, 2018, **71**(2): e1-e8.
[15] Newman DJ, Cragg GM. Natural products as sources of new drugs over the nearly four decades from 01/1981 to 09/2019 [J]. *J Nat Prod*, 2020, **83**(3): 770-803.
[16] Wagner H, Bauer R, Melchart D, *et al*. Fructus Retinervus Luffae – Sigualuo [A]. *In*: Wagner H, Bauer R, Melchart D, Xiao PG, Staudinger A. *Chromatographic Fingerprint Analysis of Herbal Medicines Volume III* [C]. Springer, Cham, 2015: 171-183.
[17] Liu J. Pharmacology of oleanolic acid and ursolic acid [J]. *J Ethnopharmacol*, 1995, **49**(2): 57-68.
[18] Liu J. Oleanolic acid and ursolic acid: research perspectives [J]. *J Ethnopharmacol*, 2005, **100**(1-2): 92-94.
[19] Sultana N, Ata A. Oleanolic acid and related derivatives as medicinally important compounds [J]. *J Enzyme Inhib Med Chem*, 2008, **23**(6): 739-756.
[20] Ayeleso TB, Matumba MG, Mukwevho E. Oleanolic acid and its derivatives: Biological activities and therapeutic potential in chronic diseases [J]. *Molecules*, 2017, **22**(11): 1915.
[21] Žiberna L, Šamec D, Mocan A, *et al*. Oleanolic acid alters multiple cell signaling pathways: Implication in cancer prevention and therapy [J]. *Int J Mol Sci*, 2017, **18**(3): 643.
[22] Shanmugam MK, Dai XY, Kumar AP, *et al*. Oleanolic acid and its synthetic derivatives for the prevention and therapy of cancer: Preclinical and clinical evidence [J]. *Cancer Lett*, 2014, **346**(2): 206-216.
[23] Zhu YM, Shen JK, Wang HK, *et al*. Synthesis and anti-HIV activity of oleanolic acid derivatives [J]. *Bioorg Med Chem Lett*, 2001, **11**(24): 3115-3118.
[24] Singh GB, Singh S, Bani S, *et al*. Anti-inflammatory activity of oleanolic acid in rats and mice [J]. *J Pharm Pharmacol*, 1992, **44**(5): 456-458.
[25] Huang ZQ, Li HL, Sun LB, *et al*. Study on inhibitive effect of oleanolic acid on transplanted hepatocarcinoma in mice [J]. *Medicinal Plant*, 2011, **2**(3): 52-54.
[26] Lee DH, Lee J, Jeon J, *et al*. Oleanolic acids inhibit vascular endothelial growth factor receptor 2 signaling in endothelial cells: Implication for anti-angiogenic therapy [J]. *Mol Cells*, 2018, **41**(8): 771-780.
[27] Ahn BZ, Sok DE. Michael acceptors as a tool for anticancer drug design [J]. *Curr Pharmaceut Des*, 1996, **2**: 247-262.
[28] Gersch M, Kreuzer J, Sieber SA. Electrophilic natural products and their biological targets [J]. *Nat Prod Rep*, 2012, **29**(6): 659-682.
[29] Zhang YY, Zhang QQ, Song JL, *et al*. Design, synthesis, and antiproliferative evaluation of novel coumarin/2-cyanoacryloyl hybrids as apoptosis inducing agents by activation of caspase-dependent pathway [J]. *Molecules*, 2018, **23**(8): 1972.
[30] Song JL, Zhang J, Liu CL, *et al*. Design and synthesis of pregnenolone/2-cyanoacryloyl conjugates with dual NF-*κ*B inhibitory and anti-proliferative activities [J]. *Bioorg Med Chem Lett*, 2017, **27**(20): 4682-4686.
[31] Fu XY, Yang YH, Li XL, *et al*. RGD peptide-conjugated selenium nanoparticles: antiangiogenesis by suppressing VEGF-VEGFR2-ERK/AKT pathway [J]. *Nanomedicine*, 2016, **12**(6): 1627-1639.
[32] Huang SW, Lien JC, Kuo SC, *et al*. PPemd26, an anthraquinone derivative, suppresses angiogenesis *via* inhibiting VEGFR2 signalling [J]. *Br J Pharmacol*, 2014, **171**(24): 5728-5742.
[33] Kowanetz M, Ferrara N. Vascular endothelial growth factor signaling pathways: therapeutic perspective [J]. *Clin Cancer Res*, 2006, **12**(17): 5018-5022.

Cite this article as: MENG Ning, XIE Hong-Xu, HOU Jia-Rong, CHEN Yan-Bin, WU Meng-Jun, GUO Yue-Wei, JIANG Cheng-Shi. Design and semisynthesis of oleanolic acid derivatives as VEGF inhibitors: Inhibition of VEGF-induced proliferation, angiogenesis, and VEGFR2 activation in HUVECs [J]. *Chin J Nat Med*, 2022, **20**(3): 229-240.